

Aluminum-Matrix Composites with Embedded Ni-Ti Wires by Ultrasonic Consolidation

Ryan Hahnen^a, Marcelo J. Dapino^a, Matt Short^b, Karl Graff^b

^a Smart Vehicle Concepts Center, The Ohio State University, Columbus, OH 43210

^b Edison Welding Institute, Columbus, OH 43221

ABSTRACT

[Smart Vehicle Workshop] This paper presents the development of active aluminum-matrix composites manufactured by Ultrasonic Additive Manufacturing (UAM), an emerging rapid prototyping process based on ultrasonic metal welding. Composites created through UAM experience process temperatures as low as 20°C, in contrast to current metal-matrix fabrication processes which require fusion of materials and hence reach temperatures of 500°C and above. UAM thus creates unprecedented opportunities to develop adaptive structures with seamlessly embedded smart materials and electronic components without degrading the properties that make embedding these materials and components attractive. This research focuses on three aspects of developing UAM Ni-Ti/Al composites which have not been accomplished before: (i) Characterization of the mechanical properties of the composite matrix; (ii) Investigation of Ni-Ti/Al composites as tunable stiffness materials and as strain sensors based on the shape memory effect; and (iii) Development of constitutive models for UAM Ni-Ti/Al composites. The mechanical characterization shows an increase in tensile strength of aluminum UAM builds over the parent material (Al 3003-H18), likely due to grain refinement caused by the UAM process. We demonstrate the ability to embed Ni-Ti wires up to 203 μm in diameter in an aluminum matrix, compared with only 100 μm in previous studies. The resulting Ni-Ti/Al UAM composites have cross sectional area ratios of up to 13.4% Ni-Ti. These composites exhibit a change in stiffness of 6% and a resistivity change of -3% when the Ni-Ti wires undergo martensite to austenite transformation. The Ni-Ti area ratios and associated strength of the shape memory effect are expected to increase as the UAM process becomes better understood and is perfected. The Brinson constitutive model for shape memory transformations is used to describe the stiffness and the strain sensing of Ni-Ti/Al composites in response to temperature changes.

Keywords: shape memory alloy, Ni-Ti, metal matrix composite, active composites, ultrasonic additive manufacturing

1. INTRODUCTION

Metal matrix composites have been investigated as a way to create multifunctionality or to achieve improved mechanical properties relative to the parent matrix material [1]. Methods for embedding long fibers, preforms, or particles generally require temperatures near or above the melting point of the matrix material. But even in powder metallurgy processes involving isostatic pressing, temperatures can reach up to 565°C [2]. This makes it challenging to embed smart materials into metallic matrices as the unique properties of smart materials are likely to degrade with exposure to high temperatures. In contrast, composites created through Ultrasonic Additive Manufacturing (UAM) experience process temperatures as low as 20°C. UAM is a new rapid prototyping technology that is used in this study to create composites consisting of an aluminum matrix and seamlessly embedded shape memory Ni-Ti wires. This research focuses on three aspects of developing UAM Ni-Ti/Al composites which have not been accomplished before: (i) Characterization of the mechanical properties of the composite matrix by means of shear, transverse tensile, and longitudinal tensile testing; (ii) Investigation of Ni-Ti/Al composites as tunable stiffness materials and as strain sensors based on the shape memory effect; and (iii) Development of constitutive models for quantifying the stiffness and stress-strain response of Ni-Ti/Al composites.

Ultrasonic Additive Manufacturing incorporates the principles of ultrasonic metal welding and subtractive processes to create metal parts with arbitrary shapes and seamlessly embedded materials [3]. UAM is a solid state process which allows joining of metallic materials far below their respective melting temperatures. Being a low-temperature process, UAM offers unprecedented opportunities to create parts with embedded smart materials (e.g., shape memory alloys, fiber

optics, polymers, etc.) and electronic components. Further, the subtractive stage integrated within the newest UAM systems allows for the simultaneous incorporation of arbitrarily shaped internal features such as cooling channels, designed anisotropies, etc.

The key features of ultrasonic metal welding are shown in Fig. 1. Ultrasonic transducers drive the transversely vibrating tip of the sonotrode which is pressed against the top work piece. This imparts a motion to the top piece and creates a relative, friction-like action at the interface of the work pieces. This relative interface motion causes shear deformations of contacting surface asperities, dispersing interface oxides and ultimately bringing clean metal-to-metal contact and adhesion between the surfaces [4].

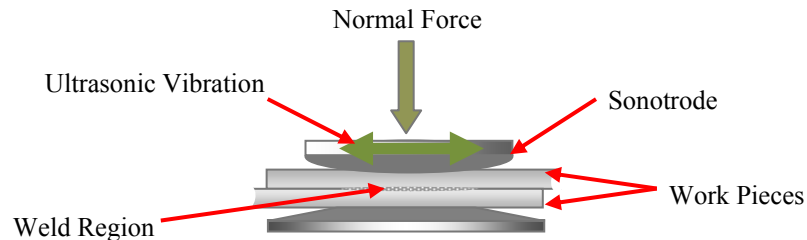


Fig. 1. Schematic representation of ultrasonic metal welding, a solid-state joining process which forms the basis for ultrasonic additive manufacturing (UAM).

Ultrasonic metal welding has been adapted into a rotating transducer, booster, and horn system for UAM, creating a new and distinct manufacturing process with capabilities not possible to achieve with conventional ultrasonic metal welding processes. As shown in Fig. 2(b)-(c), instead of a spot contact, vibrations generated by a piezoelectric ultrasonic transducer are transmitted into the parts through a rolling sonotrode. The vibrations propagate longitudinally from the transducer to the sonotrode through tuned waveguides. Normal force is applied to the vibrating sonotrode as it rolls along the work piece. The vibrations transmitted to the weld interface cause a solid-state bond between the parts. The current UAM systems achieve the most effective bonding on thin metal layers of approximately 0.006 in (152 μm) thickness. The UAM system therefore employs an automated feed mechanism for allowing successive layers of metal tapes, drawn from a continuous spool, to be bonded together for creating larger bulk builds. A subtractive CNC-based stage is also fully automatic and integrated within the UAM system (Fig. 2(a)).

UAM makes it possible to not only embed hard reinforcement materials, such as sigma fibers (TiB fibers with a tungsten core and SiC casing) but also brittle materials such as fiber optics (Fig. 3(a) and (c)). Being a solid state process, UAM has also been utilized to embed and join dissimilar materials, such as copper and aluminum (Fig. 3(b)), and to create materials with arbitrary internal spaces (Fig. 3(d)). Possibilities of advanced UAM builds include augmented structural panels with embedded reinforcement that could be monitored for damage using embedded sensors, or thermal control using embedded thermocouples for sensing with integrated internal channels for on-demand cooling at specific locations. With UAM it is possible to have a multifunctional build capable of meeting structural, sensing, motion control, and stiffness control requirements. In addition to sensors and fibers, UAM offers the opportunity to embed entire electronic components or circuit boards, allowing for sophisticated data acquisition, control, or monitoring systems to be fully integrated into a structural package. Advanced capabilities, such as reversible adhesion, in which ultrasonic bonds between metal parts are created and then separated on demand, have also been investigated using the unique abilities of UAM.

Embedding materials using UAM can be accomplished through one of two general procedures, depending on the shape and size of the embedded objects. Common to both methods, the UAM process is paused at the desired height of the embedded material. In the first, and most simple, method the embedded material is oriented as desired and the next tape layer is welded as normal. This method relies entirely upon the normal force and ultrasonic vibrations to plastically deform and flow the matrix material around the embedded object. As seen in Fig. 4, this method has proven to work well for round, small diameter Ni-Ti wires. As the wire diameter increases, more normal force and ultrasonic power are required to produce sufficient material flow to fully envelop the embedded material.

The second method of embedding involves machining a pocket in the previously consolidated layers. Once the embedded objects are placed in the machined pocket, successive tapes are welded on top to fully enclose the embedded material. This method is used for embedded materials or objects of large size or irregular shape and has been proven as a viable way of embedding sensors and electric components [5].

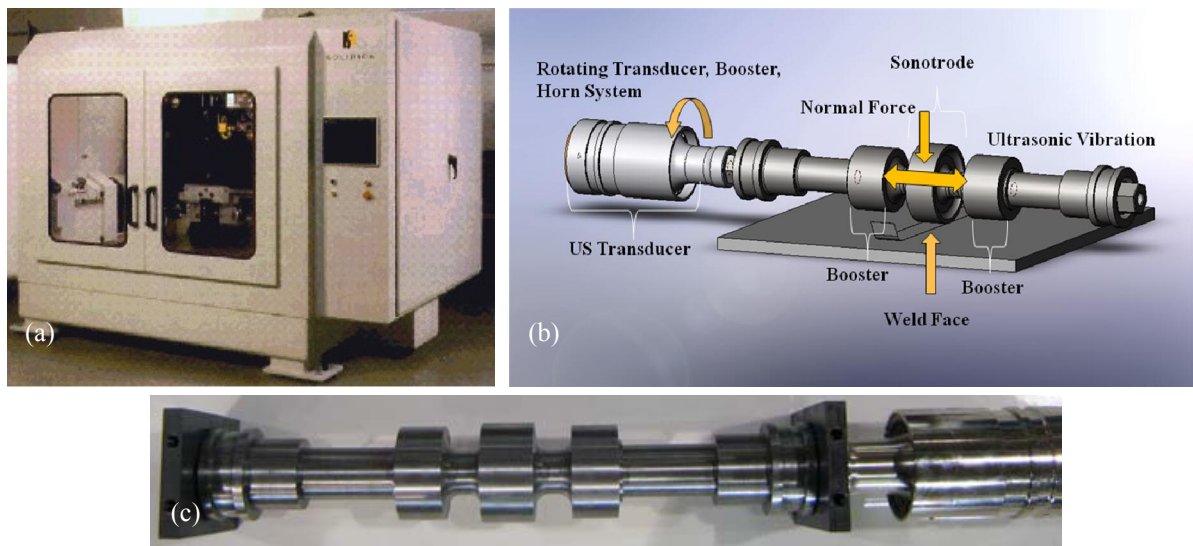


Fig. 2. (a) UAM ‘Beta’ machine used to manufacture strength testing samples. (Photograph courtesy of Solidica, Inc.) (b) In the UAM process, successive layers of metal tape are bonding together for creating metallic composites with seamlessly embedded materials and features. (c) Rotating transducer, booster and horn system used in UAM.

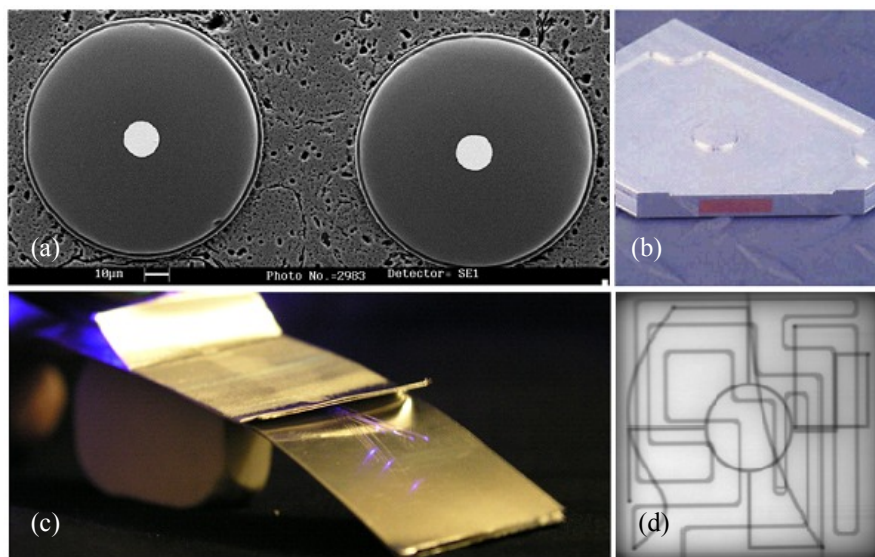


Fig. 3. (a) Micrograph of 100 mm sigma fibers embedded in aluminum. (b) Aluminum UAM build with embedded copper block. (c) Fiber optics embedded between aluminum tapes. (d) An X-ray image of a UAM build with arbitrary multi-level internal channels made using subtractive processes. (Photographs (a)-(c) courtesy of Solidica, Inc.)

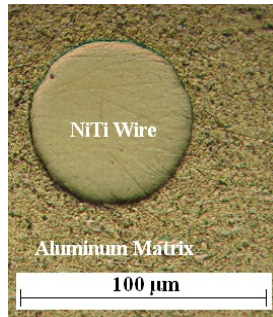


Fig. 4. Micrograph of 75 μm diameter shape memory Ni-Ti wire fully embedded in Al 3003-H18 UAM matrix utilizing only plastic flow of the matrix material.

2. METHODS

2.1 UAM sample manufacture

Samples for this research were created by welding successive layers of Al 3003-H18 tape onto an Al 3003 base plate. Al 3003-H18 is an aluminum manganese alloy that has been strain tempered and cold worked into its fully hardened condition [6]. The mechanical strength of the UAM matrix was quantified through three types of characterization: shear, transverse tensile, and longitudinal tensile. The ability of active Ni-Ti/Al composites to sense deformations and change their stiffness in response to heat was investigated analytically and experimentally.

Two active composites with 4.5% and 13.4% Ni-Ti cross sectional area ratio were constructed using a 10 kW UAM system which allows for the embedding of up to 203 μm diameter Ni-Ti wires. The two composites have eight 100 μm diameter and six 203 μm diameter wires, respectively, embedded between two aluminum tapes. The active composites were manufactured without machining recesses for the wires; the wires were embedded through plastic flow of the matrix material. Previous embedding attempts have yielded embedded fibers 100 μm in diameter without wire recesses [7]. Our new builds demonstrate an increase greater than 100% in the diameter of embedded wires relative to previous studies.

2.2 UAM matrix characterization

One of the objectives of this study is to quantify (for the first time) the mechanical properties of the aluminum matrix in UAM composites. Samples that were created for mechanical testing are identified by an indicial notation based upon the orientation of the test load relative to the direction of the ultrasonic weld and the type of applied load (Fig. 5). For this convention, a 3-D axis is oriented with the +x direction running parallel to the weld path, the +y direction parallel to the baseplate and perpendicular to the weld direction, and the +z direction starting orthogonal to the baseplate and extending upwards through the UAM layers. The first index, *i*, indicates whether the applied load is oriented along the x, y, or z axis. The second index, *j*, indicates what type of load is applied to the sample; 1 indicates a shear load, 2 indicates a tensile load, and 3 indicates a compressive load.

Shear samples (1-1) were designed to test the shear strength of a weld interface, transverse tensile samples (3-2) were designed to test the tensile strength of the samples perpendicular to the weld interface, and longitudinal tensile samples (1-2) were designed to test the sample tensile strength parallel to the ultrasonic welds. These orientations were identified as common modes of failure for long fiber reinforced matrices [8]. Three sample types constructed for material testing are shown in Fig. 6. All strength specimens were placed in a universal tension/compression testing frame and tested under displacement control. Samples were strained using a ramp input while recording the applied force. Maximum loads were used to obtain ultimate stresses and the shape of the force displacement plots was used to help characterize specimen failures.

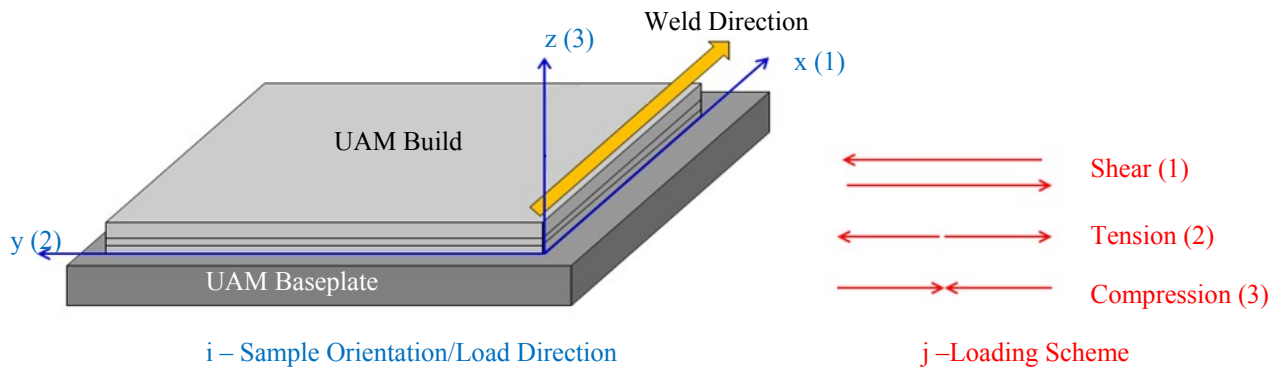


Fig. 5. Indicinal notation diagram for UAM mechanical testing samples.

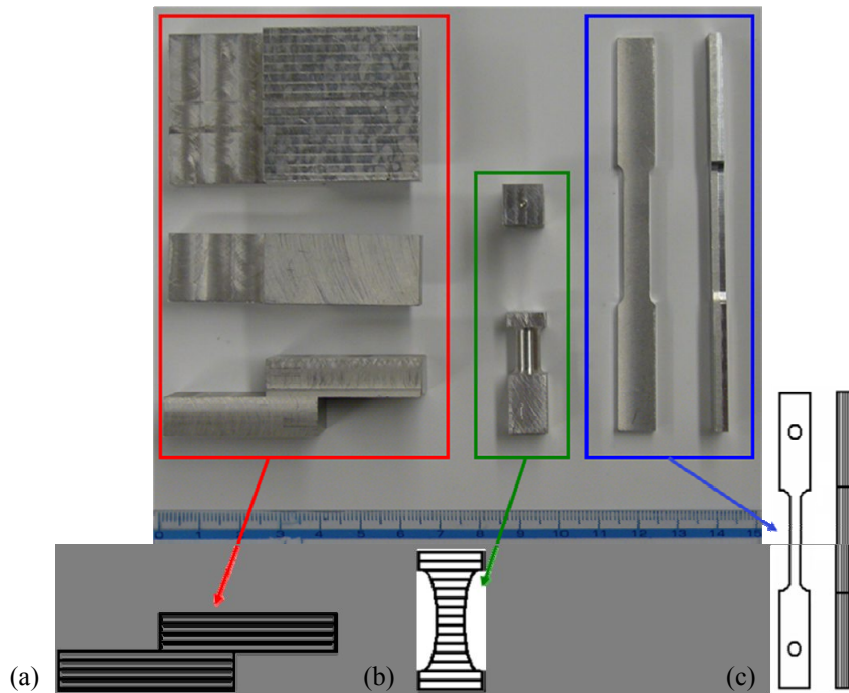


Fig. 6. UAM samples and tape diagrams: (a) UAM 1-1 sample, (b) UAM 3-2 sample, (c) UAM 1-2 sample.

2.3 Active composite characterization

Characterization of the active composites involved the creation of two models based on the 4.5% and 13.4% area ratio composites: composite strain sensing (based on resistivity change between the martensite and austenite phases) and composite stiffness characterization (based on modulus change between the martensite and austenite phases). The composite samples were machined in the shape of dog bones with a nominal gauge width of 3.18 mm and thickness of 0.46 mm. The composite with 100 μm diameter wires had a Ni-Ti area ratio of 4.5% while the composite with 203 μm diameter wires had a Ni-Ti area ratio of 13.4%.

2.3.1 Composite sensing characterization

When transforming between the martensitic and austenitic phases, Ni-Ti undergoes a change in electrical resistivity as a function of volume fraction [9]. Using this concept, an experiment was designed to investigate the change in resistance of Ni-Ti as function of stress and temperature. In conducting the Ni-Ti sensing experiment, a Ni-Ti wire was connected as part of a Wheatstone bridge and placed under mechanical and thermal loading conditions. Voltage change of the

bridge was measured using a Vishay signal conditioning amplifier. The amplifier output, proportional to the resistance of the Ni-Ti wire, was monitored while the Ni-Ti wire was thermally cycled from approximately 20°C to 160°C both unloaded and under a 12 N axial load. From the experiment, key material properties (transition temperatures, stress influence coefficients, and electrical resistivities of the austenite and martensite phases) of the Ni-Ti alloy were obtained. Using these properties, a model was created to predict the sensing performance of the Ni-Ti/Al composites.

2.3.2 Composite stiffness characterization

The stiffness of UAM composites was quantified using published material property data for both the aluminum matrix material and the Ni-Ti alloy embedded within the composite. A model was constructed to estimate the stiffness of the active composites at temperatures ranging from 20°C to 200°C. The loading conditions for the stiffness model consist of a force applied in the 1-2 orientation. This orientation resulted in the greatest strength of the matrix and placed the embedded Ni-Ti fibers directly along the load path.

Composite stiffness experiments were conducted to test the accuracy of the model and demonstrate proof of the active stiffness concept. During the stiffness experiments, both embedded composites were tested by suspending them vertically and applying a fixed static load of 20 N along the 1-2 orientation. Strain measurements were made at room temperature and again at an elevated temperature of approximately 150°C to ensure transformation of the embedded Ni-Ti. For each sample the applied load was cycled multiple times at room temperature and at elevated temperature. The displacement data from an MTS 634.31 extensometer was then used to calculate the stiffness of the sample.

3. EXPERIMENTAL RESULTS

3.1 UAM matrix characterization

All UAM 1-1 tests resulted in a linear force-displacement relationship indicating brittle fracture, as illustrated in Fig. 7. Table 1 shows an average ultimate shear strength of 52.6 MPa. The average ultimate shear strength for the UAM samples was 47.8% of that of the parent material, Al 3003-H18, which has an ultimate shear strength of 110 MPa [9]. UAM 3-2 samples behave similar to 1-1 samples, also failing in brittle fracture modes as shown in Fig. 8. The results from 3-2 samples have an average ultimate transverse tensile strength of 30.4 MPa. The strength of UAM 3-2 samples is 15.2% of the tensile strength of Al 3003-H18, which is rated at 200 MPa [9]. Unlike the other UAM samples, 1-2 samples display a plastic yielding region after the linear elastic region, as shown in Fig. 9. This is typical of aluminum alloys and also indicates that failure occurred in a ductile mode rather than the brittle mode common to 1-1 and 3-2 samples. UAM 1-2 samples exhibit an average ultimate longitudinal tensile stress of 236 MPa, 17.8% greater than the solid parent material. This is a departure from both the 1-1 and 3-2 samples in which the obtained failure stresses are significantly lower than the rated strength of the parent material. The observed increase in tensile strength over the parent material likely due to grain refinement of the aluminum tapes as a result of the UAM process. The UAM sonotrode has a texture which helps to transfer ultrasonic vibrations to the weld interface. The combination of mechanical deformations caused by sonotrode texture was well as the ultrasonic vibrations is thought to be the cause of the finer aluminum grain structure and subsequent strengthening of the material [10].

Table. 1. Comparison of Al 3003 H-18 base material and UAM material properties.

Strength	Al 3003-H18 [MPa] [6]	UAM [MPa]	Percent of Solid Strength
Ultimate shear (1-1 mode)	110	52.6	47.8%
Ultimate transverse tensile (3-2 mode)	200	30.4	15.2%
Ultimate longitudinal tensile (1-2 mode)		236	117.8%

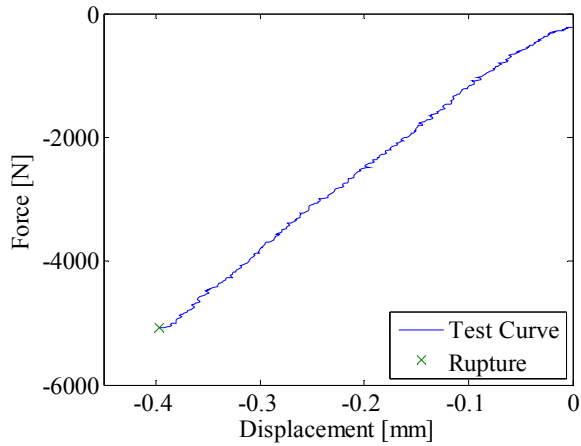


Fig. 7. UAM 1-1 sample force versus displacement curve indicating brittle failure of the sample.

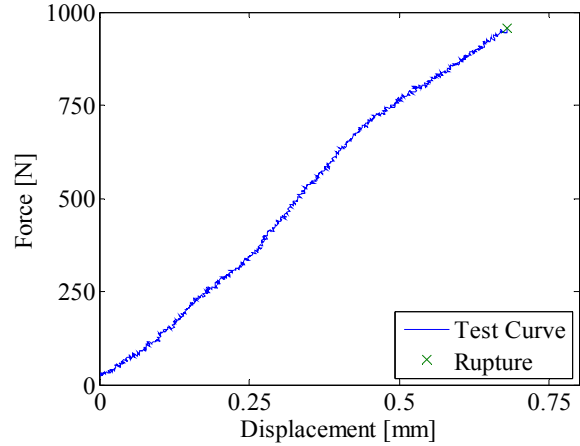


Fig. 8. UAM 3-2 sample force versus displacement curve indicating brittle failure of the sample.

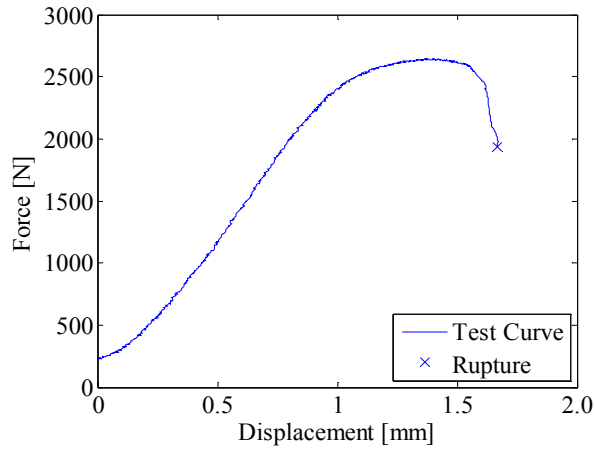


Fig. 9. UAM 1-2 sample force versus displacement curve showing significant plastic yielding, indicating ductile failure of the sample.

3.2 Active composite characterization

3.2.1 Active composite sensing characterization

As shown in Fig. 10, the resistance response of the Ni-Ti wire is such that regardless of load, the wire exhibits a change in resistance of -3% after transformation to the austenite phase from the room temperature martensite phase. The effect of load is to shift the austenite start and finish temperatures, changing the temperature at which the M-A transition and subsequent large resistance drop take place. For this particular alloy, the load appears to have little effect on the temperature range at which the A-M transition occurs. The material used in this experiment (90°C Flexinol) is the same alloy used in the UAM composites. From these experiments, the transition temperatures, their stress influence coefficients, and electrical resistivities were determined for use in the model, as seen in Table 2. The value for C_M was approximated such that load has little effect on the A-M transition in the following Ni-Ti models.

A model for Ni-Ti composite sensing capabilities was developed which quantifies the resistivity of the embedded Ni-Ti as a function of volume fraction and temperature. In the model, the electrical resistivities of both phases are first adjusted

for temperature using their respective temperature coefficients [11]. Once temperature adjusted resistivities for the austenite and martensite phases are found, the total Ni-Ti resistance is calculated in a manner similar to calculating the elastic modulus using volume fraction [12]. The resistivity of the Ni-Ti wire is modeled by

$$\rho_{NiTi}(\xi, T) = \xi [\rho_M + \kappa_M (T - T_o)] + (1 - \xi) [\rho_A + \kappa_A (T - A_f)]. \quad (1)$$

For modeling the composite structures, the resistances of the Ni-Ti and aluminum regions are calculated individually through the relations

$$R_{NiTi} = \frac{\rho_{NiTi} L}{A}, \quad (2)$$

and

$$R_{Al} = \frac{\rho_{Al} L}{A}. \quad (3)$$

The total composite resistance is then calculated as a parallel resistor pair,

$$R_{comp} = \left[\frac{1}{R_{Al}} + \frac{1}{R_{NiTi}} \right]^{-1}, \quad (4)$$

whereas the change in resistance is calculated by

$$\Delta R_{comp} \% = \frac{R_{comp}(T) - R_{comp}(20^\circ C)}{R_{comp}(20^\circ C)} \times 100. \quad (5)$$

Material properties not found in the previous experiment were taken from literature sources as shown in Table 3.

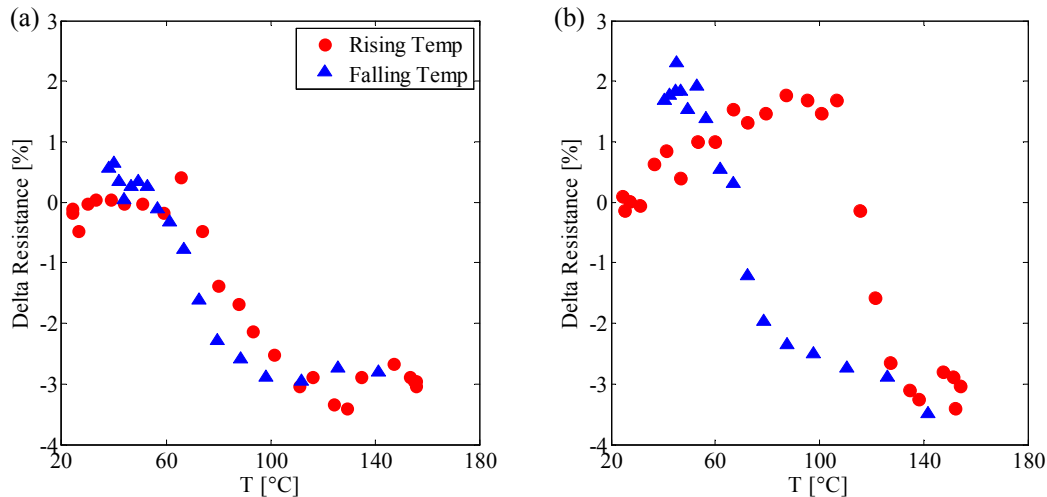


Fig. 10. Experimental Ni-Ti resistance response showing the change in electrical resistance versus temperature. (a) Unloaded case; (b) 12 N load.

Table. 2. Material properties of 90°C Flexinol as derived from experiments

Property	Description	Value
M_f	Martensitic finish temperature	55 °C
M_s	Martensitic start temperature	90 °C
A_s	Austenitic start temperature	65 °C
A_f	Austenitic finish temperature	100 °C
C_A	Austenitic stress influence coefficient on austenite temperatures	3 MPa/°C
C_M	Martensitic stress influence coefficient on martensite temperatures	1000 MPa/°C
ρ_A	Austenite electrical resistivity	0.92 $\mu\text{Ohm}\cdot\text{m}$
ρ_M	Martensite electrical resistivity	1.07 $\mu\text{Ohm}\cdot\text{m}$

Table. 3. Additional material properties used for sensing and stiffness models.

Property	Description	Value
κ_A [11]	Austenite resistivity temperature coefficient	0.50 nOhm-m/°C
κ_M [11]	Martensite resistivity temperature coefficient	1.75 nOhm-m/°C
E_A [13]	Austenite elastic modulus	67 GPa
E_M [13]	Martensite elastic modulus	26 GPa
$E_{Al}(20^\circ\text{C})$ [14]	Aluminum elastic modulus at 20°C	68 GPa
$E_{Al}(100^\circ\text{C})$ [14]	Aluminum elastic modulus at 100°C	66 GPa
$E_{Al}(150^\circ\text{C})$ [14]	Aluminum elastic modulus at 150°C	63 GPa

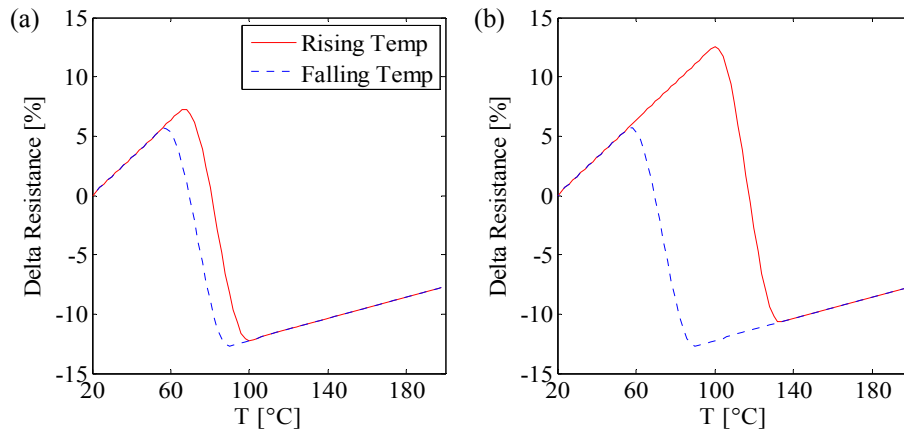


Fig. 11. Ni-Ti resistance model describing the change in electrical resistance versus temperature. (a) Unloaded case; (b) 12 N load.

As shown in Fig. 11, the Ni-Ti wire resistance model describes the overall shape of the experimental data and returns the same order of magnitude for change in resistance change observed in the sensing experiments. The Ni-Ti resistance model was incorporated into the Ni-Ti/Al composite model which gives the calculated composite resistance change as a function of temperature (Fig. 12). The composite sensing model indicates that an approximate -1% change in resistance is expected for the 4.5% Ni-Ti area ratio composite while the 13.4% Ni-Ti area ratio composite is expected to experience a -3% change in resistance over the temperature range from 20°C to 200°C with no axial load.

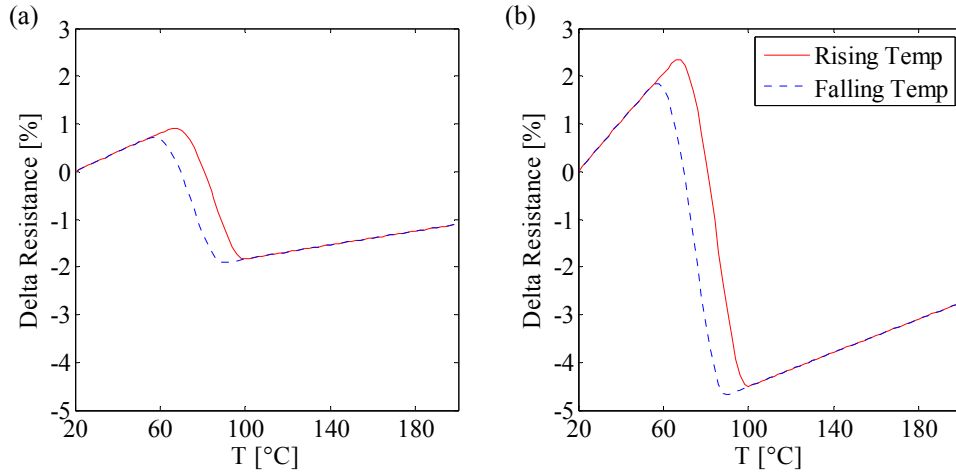


Fig. 12. Resistance model results describing the composite change in resistance versus temperature.
 (a) 4.5% Ni-Ti area ratio composite (b) 13.4% Ni-Ti area ratio composite.

3.2.2 Active composite stiffness characterization

For long fiber reinforced matrices, stiffness is calculated as a rule of mixtures [7],

$$k_{comp} = \frac{(E_{NiTi}A_{NiTi} + E_{Al}A_{Al})}{L} \quad (6)$$

The elastic modulus of aluminum is linearly interpolated with temperature using modulus values at 20°C, 100°C, and 150°C, seen in Table 3. The elastic modulus of Ni-Ti is calculated as a function of volume fraction using the Brinson model, which predicts the following relation between volume fraction and modulus [12],

$$E_{NiTi} = \xi E_M + (1 - \xi) E_A \quad (7)$$

A maximum percent change in stiffness is calculated by difference in composite stiffness when the embedded Ni-Ti is fully austenitic and when it is fully martensitic, normalized by the martensitic composite stiffness,

$$\Delta k \% = \frac{k_{comp}(T) - k_{comp}(20^\circ C)}{k_{comp}(20^\circ C)} \times 100 \quad (8)$$

The model results for expected stiffness change are shown in Fig. 13. The modeling of the two different composites shows that the sample with 100 μm diameter wires does not have a sufficient Ni-Ti area ratio to overcome the softening of aluminum with increasing temperature. This results in a net softening of the composite soon after the M-A transition temperature. The build with 203 μm diameter wires is able to offset stiffness lost by the matrix through stiffening associated with the M-A transition of Ni-Ti. Further analysis of the model will provide a critical area ratio which gives a minimum percentage of embedded Ni-Ti to counteract the softening of the aluminum matrix at a given temperature. Though the model predicts only the 13.4% Ni-Ti area ratio composite will experience an increase over room temperature

stiffness, both composites are expected to be stiffer than a solid aluminum piece of the same dimensions at temperatures above A_f . The results from composite stiffness testing experiments are shown in Table 4. As predicted by the model, the 4.5% area ratio build experiences a decrease in stiffness after the M-A transition of the embedded wire. The 13.4% area ratio composite also correlates with the increase in stiffness predicted by the model. The 4.5% Ni-Ti area ratio composite experiences a 6% reduction in stiffness while the 13.4% Ni-Ti area ratio composite exhibits a 5.5% increase in stiffness.

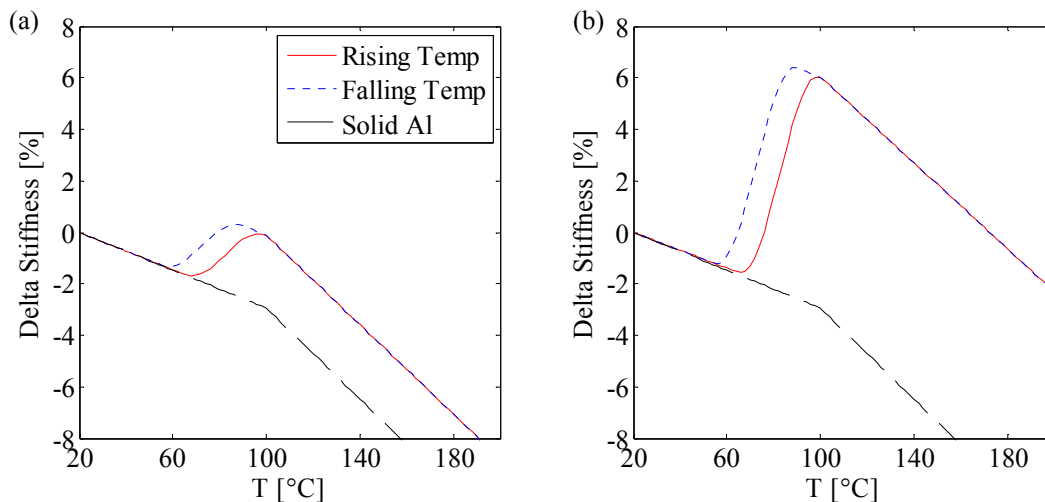


Fig. 13. Ni-Ti composite stiffness versus temperature. (a) 4.5% Ni-Ti area ratio composite. The model indicates there is insufficient NiTi to offset the softening of the matrix with increasing temperature. (b) 13.4% Ni-Ti area ratio composite. The model indicates an increase in composite stiffness with temperature up to approximately 180°C. Both models show an increased stiffness over solid aluminum in the same geometry after the M-A transition.

Table 4. Composite stiffness testing results

Ni-Ti Area Ratio	Ni-Ti Phase	Average k [N/m]	Percent Stiffness Change
4.5%	Martensite	2.84E+06	-6.0%
	Austenite	2.67E+06	
13.4%	Martensite	1.10E+06	5.5%
	Austenite	1.16E+06	

4. SUMMARY

A better understanding of aluminum-matrix composites made using UAM has been attained through mechanical testing of the matrix using shear, transverse tensile, and longitudinal tensile tests. Aluminum 3003-H18 samples made through UAM have been found to be nearly 18% stronger than solid parent material in the 1-2 direction while significantly weaker than the parent material in the 1-1 and 3-2 directions. The strengthening is likely due to grain refinement caused by the combination of ultrasonic vibrations and horn texture.

The resistance of a specific Ni-Ti alloy (90°C Flexinol) was experimentally determined as a function of axial load and temperature. These results were used to formulate a constitutive model that describes the ability of Ni-Ti/Al composites to be used as load or strain sensors. We demonstrate the ability to embed Ni-Ti wires up to 203 μm in diameter in an aluminum matrix, compared with only 100 μm in previous studies. It is expected that higher ultrasonic power relative to the 10 kW system used in this study will allow for the embedding of larger diameter wires.

Two Ni-Ti/Al composites were used to demonstrate the change composite stiffness with temperature. It was found through modeling, and confirmed through experimental measurements, that there is a critical area ratio above which the stiffness of an active composite will increase with temperature. Experiments with a 13.4% Ni-Ti area ratio Ni-Ti/Al composite have demonstrated a stiffness increase at elevated temperatures of 5.5% over the stiffness of the composite at 20°C. The experiments suggest the embedding of Ni-Ti can be used not only for sensing or stiffness control but also to create composites with invariant shape when subjected to temperature changes. This will necessitate accurate models for determining the exact area ratio of Ni-Ti required to achieve invariance over a certain temperature range. These materials could prove useful for applications in which critical tolerances wish to be maintained while the temperature of the system changes, or as a means to match the effective coefficient of thermal expansion of the composite to that of other materials. Future Ni-Ti/Al composite builds will have a primary design goal of increasing the Ni-Ti area ratio in order to achieve larger composite stiffness and resistance changes, thereby increasing the effectiveness of the composites as active structures.

The focus of future work will be on characterizing and modeling the interface between Ni-Ti wires and the aluminum matrix in active UAM composites. The interface characterization will be integrated into the current sensing and stiffness models to more accurately represent the mechanics of the composites. A new experimental setup will also be developed to provide continuous loading of Ni-Ti/Al composites while providing increased temperature control during experimental tests.

ACKNOWLEDGEMENTS

Financial support for this research was provided by the Smart Vehicle Concepts Center (www.SmartVehicleCenter.org), a National Science Foundation Industry/University Collaborative Research Center, and by the Ohio State University through a Smart Vehicle Concepts Graduate Fellowship.

REFERENCES

- [1] Krainer, K., [Metal Matrix Composites], Wiley-Vch Wevlag GmbH & Co., Weinheim, 2-52 (2006).
- [2] Chawla, N., "Metal Matrix Composites in Automotive Applications," *Advanced Materials and Processes*, 29-31 (2006).
- [3] Graff, K., [New Developments in Advanced Welding], Woodhead Publishing Limited, Cambridge, 241 (2005).
- [4] De Vries, E., "Mechanics and Mechanisms of Ultrasonic Metal Welding," Ph.D. Thesis, The Ohio State University, (2004).
- [5] Siggard, E., "Investigative Research into the Structural Embedding of Electrical and Mechanical Systems using Ultrasonic Consolidation," M.S. Thesis, Utah State University, (2007).
- [6] Kutz, M., [Handbook of Material Selection], John Wiley and Sons, Inc., New York, 89-134 (2002).
- [7] Kong, C., Soar, R., "Fabrication of metal-matrix composites and adaptive composites using ultrasonic consolidation process," *Materials Science and Engineering A*, 412, 12-18 (2005).
- [8] Clyne, T., Withers, P., [An Introduction to Metal Matrix Composites], Davis, E., Ward, M., Cambridge University Press, Cambridge, 12-14 (1993).
- [9] Gori, F., Carnevale, D., Doro Atan, A., Nicosia, S., Pennestri, E., "a New Hysteretic Behavior in the Electrical Resistivity of Flexinol Memory Alloys Versus Temperature," *International Journal of Thermophysics*, 27(3), 866-879 (2006).
- [10] Johnson, K., "Interlaminar Subgrain Refinement in Ultrasonic Consolidation," Ph.D. Thesis, Loughborough University, (2008).
- [11] Matsumoto, H., "Electrical resistivity of NiTi with a high transformation temperature," *Journal of Materials Science Letters*, 11, 367-368 (1992).
- [12] Hartl, D., Lagoudas, D., [Shape Memory Alloys], Springer Science and Business Media, LLC, New York, 53-119 (2008).
- [13] Dynalloy, Inc., 1070 Commercial Street, Suite No. 110, San Jose, California 95112. <http://www.dynalloy.com>, (2008).
- [14] Kaufman, J., "Aluminum Alloy Database," Knovel, http://knovel.com/web/portal/browse/display?_EXT_KNOVEL_DISPLAY_bookid=844&VerticalID=0, (2004).